

AD-750 329

DEFORMATION AND FRACTURE OF TANK BOTTOM  
HULL PLATES SUBJECTED TO MINE BLAST

Donald F. Haskell

Ballistic Research Laboratories  
Aberdeen Proving Ground, Maryland

1972

AD 750 329

DISTRIBUTED BY:

**NTIS**

National Technical Information Service  
U. S. DEPARTMENT OF COMMERCE  
5285 Port Royal Road, Springfield Va. 22151

57

HASKELL

AD 750 329

AD 750329

DEFORMATION AND FRACTURE OF TANK BOTTOM  
HULL PLATES SUBJECTED TO MINE BLAST

DONALD F. HASKELL, Ph.D.  
VULNERABILITY LABORATORY  
BALLISTIC RESEARCH LABORATORIES  
ABERDEEN PROVING GROUND, MARYLAND

I. INTRODUCTION

The vulnerability analyst, munitions designer, and armored vehicle designer need a methodology for determining the effects of mine blast attack on the integrity of armored vehicle hull bottom plates. In the past the information required to assess mine-tank bottom encounters had to be obtained by rather expensive and time consuming test programs - analytical methods to develop this information were not available. This situation was caused by the very complicated nature of the problem.

To avoid these complications and yet achieve simple but relevant and reasonably accurate characterizations of the subject problems, an approximate energy method approach was selected. In this method, based on the law of conservation of energy, the energy delivered to the armor plate by the blast is equated to the strain energy absorbed by the plate in reaching its final deformed shape at the end of the blast. Fracture is assumed to occur when the maximum normal tensile strain in the plate reaches the tensile failure strain of the plate material (a value easily obtained by standard tensile test).

Figure 1 illustrates the specific mine-plate configuration treated in this study. As shown, the plate is a flat, rectangular plate representative of the bottom hull plate of typical armored vehicles. The width, length, and thickness of the plate are  $a$ ,  $b$ , and  $h$ , respectively. The plate is assumed to be simply supported around its edges with little in-plane constraint. Located directly below the plate center at standoff  $R$  is the mine of weight  $W$ . As in combat, the top of the mine is either flush with the surface of the ground or shallow-buried. Under action of the mine blast the plate deforms into the final pattern with amplitude  $A$  shown schematically in Figure 1. This final deformation pattern, as indicated by available measured deformation from plate blast tests (Ref. 1) shown in Figure 2, is closely represented by a cosine function with its origin at the plate center. The small amount of soil atop the shallow-buried mine is assumed to have negligible effect on this damage. All the damage is

Reproduced by  
NATIONAL TECHNICAL  
INFORMATION SERVICE  
U.S. Department of Commerce  
Springfield VA 22151

For public use...  
distribution is unlimited

Begin-30

15

HASKELL

attributed to the effects of free-air blast. Although the influence of both mine shape and explosive fill on blast energy per unit area can be easily handled by the blast treatment developed here, these effects have not been taken into account in comparing the theoretical predictions with test results. The mine blast energy per unit area (mine blast wave energy flux density) is calculated as usual by neglecting the excess particle velocity or afterflow left by the outgoing spherical wave and the relationship between normally reflected peak pressure and time in this wave is characterized by the widely used, empirical Friedlander equation.

The general mechanical behavior of the plate material is approximated by a rigid-linear work hardening stress-strain relationship with independent components in the principal directions. Because the work hardening portion of the energy absorption capacity of typical armor plate materials is small compared to the rigid plastic portion, as illustrated schematically by Figure 3, the plate behavior is further idealized as rigid-plastic. In Figure 3  $U_E$ ,  $U_{RP}$ , and  $U_{WH}$  are the elastic, rigid-plastic, and work hardening portions of the material strain energy density and  $F_U$ ,  $F_Y$ ,  $\epsilon_Y$ , and  $e_F$  are the ultimate strength, yield strength, yield strain, and failure strain, respectively. This allows the plate strain energy to be reduced to a simple expression which, when combined with the mine blast energy in the conservation of energy law, yields explicit expressions for maximum transverse plate deformation and the plate thickness at which fracture occurs.

By treating the plate as a membrane, the large deformations experienced by mine blast attacked plates are incorporated in a general expression for the plate strain energy. This general plate strain energy expression is particularized for the deformation analysis by disregarding in-plane displacements and for the fracture analysis by neglecting transverse displacements. In addition, the fracture analysis is further simplified by taking the displacement component amplitudes in the two principal in-plane directions to be equal.

The result of this treatment is a simple method for rapidly predicting, with reasonable accuracy and without recourse to a high speed electronic digital computer, the deformation and fracture characteristics of armored vehicle hull bottom plates attacked by blast type mines. The particular equations developed should be particularly useful for quick vulnerability estimates and in the initial design phases of land mines and most armored vehicle design projects. Furthermore, the method employed in developing these equations is general in nature and, as such, is applicable to a wide range of problem areas.

## II. DESCRIPTION OF AVAILABLE TESTS

All the data presented in this report were obtained from available test results and battle damage records. The data consist of results from armor plate - mine blast tests performed at Aberdeen Proving Ground as well as combat damage data collected by the Battle Damage Assessment and Reporting Program (BDARP) teams operating in

## HASKELL

South Vietnam. To compile the APG data a detailed search was performed of all APG/D&PS and APG/MTD armor firing records from 1942 to 1971. The data from this survey used in this report represents approximately 107 plate tests. The BDARP data used in this report were obtained from a review of 244 mine-armored vehicle incidents compiled by the BDARP teams.

The plates tested included 5083 aluminum and rolled homogeneous steel armor plate. Charge weight ranged from 2.5 to 25 lb with a constant standoff and burial depth of 17 in. and 3 in., respectively. Since mechanical properties test results for each of the plates tested were not available, estimates of the necessary parameters were obtained from the material specifications. Yield strength and failure strain for the 5083 aluminum alloy plates were obtained from HDBK 23 specifications. In regard to the steel armor plate, measured or specified hardness values were converted to yield strength and failure strain by means of well known relations (Ref. 2). The steel plates ranged in thickness from 3/4 in. to 1-1/2 in. while thickness of the aluminum plates ranged from 3/4 in. to 3 in. All plates were essentially the same size - either 40 in. by 65 in. or 44 in. by 65 in. All the aluminum plates were apparently of the same strength and ductility whereas the steel plates ranged in strength and ductility from 90,000 psi to 172,000 psi and 0.15 in/in. to 0.23 in/in., respectively.

## III. DEVELOPMENT OF ANALYSES

GENERAL. Both deformation and fracture treatments in this investigation are based upon an approximate semi-inverse energy method of analysis. In this method the mine blast-plate response process is characterized by the law of conservation of energy. For the subject problem this law may be stated in the following manner: the work done by the mine blast equals the sum of the kinetic energy and strain energy stored in the system. It may be shown that the system kinetic energy is negligible compared to the energy from the mine and the strain energy absorbed by the armor plate. Consequently, the deformation problem reduces to formulation of mine blast and plate strain energy expressions which, when equated according to the law of conservation of energy, yield an explicit expression for plate deformation.

Plate fracture is treated in a similar manner. Mine blast energy delivered to the plate is equated to the strain energy absorbed by the plate up to the point of fracture. Fracture is characterized by a maximum normal strain criterion. The end result is an explicit equation for the thickness at which the plate will fracture.

BLAST CHARACTERIZATION. For convenience and to provide approximate correspondence to actual test results, the mine blast is assumed to deform the plate into the following pattern:

$$w = A \cos \frac{\pi x}{a} \cos \frac{\pi y}{b} \quad (a)$$

$$u = B \sin \frac{\pi x}{a} \cos \frac{\pi y}{b} \quad (b) \quad (1)$$

$$v = C \cos \frac{\pi x}{a} \sin \frac{\pi y}{b} \quad (c)$$

## HASKELL

The energy from the mine that produces this deformation is taken as simply the mine blast energy flux density multiplied by the area of the plate:

$$E = a b E_m \quad (2)$$

where

$E$  = work done on the plate by the energy in the blast wave, in-lb

$E_m$  = mine blast energy flux density, in-lb/in.<sup>2</sup>

The mine blast flux density is the energy flow across unit area of a fixed surface normal to the direction of propagation and is defined as follows:

$$E_m = \frac{1}{c_o \rho_o} \int_0^t p^2 dt \quad (3)$$

where

$c_o$  = sonic velocity, in/sec

$\rho_o$  = air mass density, lb sec in.<sup>-4</sup>

$p$  = normally reflected pressure, psi

$t$  = time from occurrence of the peak reflected pressure, sec

The typical blast wave pressure-time history may be expressed by the Friedlander equation:

$$p = P \left( 1 - \frac{t}{\Delta t} \right) e^{-\frac{t}{\Delta t}} \quad (4)$$

where

$P$  = peak reflected pressure, psi

$e$  = base of the natural system of logarithms

$\Delta t$  = time duration of the positive normally reflected pressure, sec

Substitution of the pressure-time relation, Equation 4, into the energy flux density definition, Equation 3, and subsequent integration over the time duration of the normally reflected pressure,  $\Delta t$ , results in the relation

$$E_m = \frac{1-e^{-2}}{4c_o \rho_o} P^2 \Delta t \quad (5)$$

An approximate empirical relationship for mine blast energy flux density fitted to this relation for free air blast at sea level is

$$E_m = 109.04 \times 10 W^{1/3} \left( \frac{R}{W^{1/3}} \right)^{-1.747}, \text{ in-lb/in.}^2 \quad (6)$$

It is included here because it provides (as Equation 5 doesn't) a direct relation between energy flux density and the practical factors charge weight  $W$  and standoff  $R$ .

61

HASKELL

Equation 6 yields results that are higher than Equation 5 for scaled standoff below 5.1 in/lb<sup>1/3</sup> and above approximately 14.5 in/lb<sup>1/3</sup>, whereas between these scaled standoffs, it yields results lower than Equation 5. The maximum errors of Equation 6 over the practical mine-tank encounter range vary from +17 percent to -18 percent to +11 percent at R/W<sup>1/3</sup> = 3.86, 9.94, and 17 in/lb<sup>1/3</sup>, respectively. This scaled standoff range corresponds, for example, to a 30 lb mine at approximately 12 in. standoff up to a 2.5 lb mine at 24 in. standoff, respectively. At scaled standoffs beyond this range the approximate empirical expression, Equation 6, increasingly overestimates the mine blast energy flux density. In this case, the original expression Equation 5 should be employed for more accurate results.

MAXIMUM TRANSVERSE PLATE DEFORMATION. The maximum transverse plate deformation A (see Figure 1) is obtained by a semi-inverse approach. With the desired deformation amplitude A as an unknown parameter, the mine blast energy required to deform the plate the amount A is set equal to the strain energy absorbed by the plate in reaching this final deformed configuration. The resulting equation of mine blast energy and plate strain energy is then solved for the deformation A.

A general expression for the strain energy of deformation of a flat plate U is

$$\bar{U} = \iiint \left( \sigma_x e_x + \sigma_y e_y + \sigma_{xy} e_{xy} \right) dx dy dz \quad (7)$$

where  $\sigma_x, \sigma_y, \sigma_{xy}$  are the normal and shear stresses in the x and y plane of the plate and  $e_x, e_y, e_{xy}$  are the strains in the plane of the plate with dx dy dz an incremental volume in the plate. Since the mine blast attack produces gross deformation throughout the plate the stress-strain relations are taken as follows:

$$\begin{aligned} \sigma_x &= F_y + \bar{E} e_x \\ \sigma_y &= F_y + \bar{E} e_y \\ \sigma_{xy} &= S_y + \bar{G} e_{xy} \end{aligned} \quad (8)$$

where  $F_y$  and  $F_u$  are tensile yield and ultimate strengths, respectively,  $S_y$  and  $S_u$  are shear yield and ultimate strengths, respectively,  $e_F$  = tensile normal failure strain,  $\gamma_F$  = shear failure strain,

$$\bar{E} = \frac{F_u - F_y}{e_F}$$

and

$$\bar{G} = \frac{S_u - S_y}{\gamma_F}$$

HASKELL

Substitution of the stress-strain relations, Eq. 8, into the plate strain energy equation, Eq. 7 yields

$$\bar{U} = \int \int \int \left( F_y e_x + \bar{E} e_x^2 + F_y e_y + \bar{E} e_y^2 + S_y e_{xy} + \bar{G} e_{xy}^2 \right) dx dy dz \quad (9)$$

In this equation the work hardening contribution to the plate strain energy consists of those terms containing  $\bar{E}$  and  $\bar{G}$ . This work hardening portion of the total plate strain energy is small (5 percent and 16 percent for steel and aluminum armor plate, respectively) and hence is neglected in comparison to the rigid-plastic portion. Consequently, by assuming that the displacements  $u$ ,  $v$  and  $w$  are constant through the plate thickness and substituting the following strain-displacement relations for large plate deformation into Eq. 9:

$$\begin{aligned} e_x &= u' + \frac{1}{2} w'^2 \\ e_y &= v' + \frac{1}{2} w'^2 \\ e_{xy} &= u' + v' + w'w' \end{aligned}$$

where for convenience in notation  $( )' = \frac{\partial ( )}{\partial x}$  and  $( ) \cdot = \frac{\partial ( )}{\partial y}$  an expression for the rigid-plastic plate strain energy,  $\bar{U}_{RP}$ , is obtained:

$$\bar{U}_{RP} = h \int_{-\frac{a}{2}}^{\frac{a}{2}} \int_{-\frac{b}{2}}^{\frac{b}{2}} \left[ F_y \left( u' + \frac{1}{2} w'^2 + v' + \frac{1}{2} w'^2 \right) + S_y \left( u' + v' + w'w' \right) \right] dx dy \quad (10)$$

This relation may be further simplified by neglecting the in-plane displacements  $u$  and  $v$ . Utilizing this simplification, an expression for the major portion of the strain energy absorbed by the plate in deforming to a maximum amplitude  $A$  can be obtained by substituting the derivatives of the transverse deflection  $w$  from Equation 1a into Eq. 10. After the resulting terms are multiplied as required, and then integrated, the approximate plate strain energy can be reduced to

$$\bar{U} = \left[ \frac{\pi^2}{8} \left( \frac{a^2 + b^2}{ab} \right) F_y h \right] A^2 \quad (11)$$

Since the basis for this semi-inverse energy method is conservation of energy, the deformation can be obtained by equating Equations 2 and 11 and solving the resultant equation for  $A$ :

$$A = \frac{\sqrt{8}}{\pi} \left[ \frac{a^2 b^2}{a^2 + b^2} \frac{E_m}{F_y h} \right]^{1/2} \quad (12)$$

where  $E_m$  is given either by Equation 5 or the approximate expression of Equation 6. Equation 12 indicates that maximum transverse deformation depends on the size and shape of the plate, is directly

63

HASKELL

proportional to the square root of the mine blast energy and is inversely proportional to the square root of the plate's yield strength and thickness.

PLATE FRACTURE. The conservation of energy principle is applied to determine the conditions for plate fracture in a manner similar to its use in predicting deformation. For plate fracture the principle can be stated as follows: fracture, or rupture, occurs when the blast energy from the mine equals the maximum strain energy which can be absorbed by the plate. This maximum strain energy that can be absorbed by the plate is determined by the tensile normal failure strain of the material.

An approximate expression for strain energy can be obtained by assuming the plate to behave as a rigid-plastic material as given by Equation 10. Furthermore, if the transverse displacement is neglected, Equation 10 yields the following approximate strain energy expression which leads to a particularly simple formulation for fracture thickness:

$$\bar{U} = F_y h \int_{-\frac{a}{2}}^{\frac{a}{2}} \int_{-\frac{b}{2}}^{\frac{b}{2}} (u' + v') dx dy + S_y h \int_{-\frac{a}{2}}^{\frac{a}{2}} \int_{-\frac{b}{2}}^{\frac{b}{2}} (u' + v') dx dy \quad (13)$$

After the derivatives of u and v from Equation 1 are substituted into this equation and the integration is performed, the strain energy with  $C = kB$  becomes

$$\bar{U} = \frac{4}{\pi} F_y h (b + ka) B \quad (14)$$

and since the chosen basis for developing a fracture criterion is that the mine blast energy is equal to the plate strain energy absorbed to the point of rupture, the strain energy given by Eq. 14 is set equal to the mine blast energy:

$$a b E_m = \frac{4}{\pi} F_y h_F (b + ka) B, \quad (15)$$

where  $h_F$  is the plate thickness at which fracture occurs. This expression is related to the point of rupture, the normal failure strain of the plate material, by the parameter B, the strain amplitude in the x-direction of the plate. Since maximum strain occurs at  $x = y = 0$ , it can be shown that

$$B = \frac{a}{\pi} e_F \quad (16)$$

Substitution of this expression for B into Equation 15 and rearrangement results in the following relation for fracture thickness:

$$h_F = \frac{\pi^2}{4} \frac{E_m}{\left(1 + \frac{a}{b}\right) F_y e_F} \quad (17)$$

HASKELL

where the term  $F_y e_F$  is recognized as the plate material rigid-plastic energy absorption capacity  $U_{RP}$  and, for simplicity, it has been assumed that  $k = 1$ .

This relation indicates that the thickness at which a plate will fracture is dependent upon its shape, is directly proportional to the mine blast energy flux density, and inversely proportional to its plastic strain energy absorption capacity i.e., toughness.

#### IV. CORRELATION OF ANALYSIS AND TEST RESULTS

DEFORMATION CORRELATION. The test and analytical results are plotted in Figure 4. In this figure the test data have been plotted as reduced deformation amplitude  $A$  defined by:

$$\bar{A} = \frac{A}{\frac{\sqrt{8}}{\pi} \left( \frac{a^2 b^2}{a^2 + b^2} \frac{1}{F_y h} \right)^{1/2}} \quad (18)$$

versus mine blast energy flux energy  $E_m$  calculated by Eq. 5. As may be seen from the figure, plate deformation predicted by the present theory is higher than would be obtained in practice. The average positive error between predictions of Eq. 12 and the test results is 26 percent and the average negative error is 8 percent with the overall average error +18 percent. The average absolute error is 21 percent. If a conservative method for predicting deformation is desired the equation corresponding to either of the  $2\sigma$  limits could be employed. For example, use of the upper  $2\sigma$  curve to predict deformation would yield results that 95 percent of the time are higher than would be obtained in actual practice.

Equation 12 may be rewritten in the following manner to allow direct computation of the theoretical maximum plate deformation, the mean value as obtained by test or the  $\pm 2\sigma$  probability limits of the maximum plate deformation:

$$A = \frac{\sqrt{8}}{\pi} \left( \frac{a^2 b^2}{a^2 + b^2} \frac{1}{F_y h} \right)^{1/2} E_m^q \quad (19)$$

where

- $q = 0.5$  from theory
- $= 0.4834$  for test data mean
- $= 0.5188$  for the  $+2\sigma$  deformation limit
- $= 0.4319$  for the  $-2\sigma$  deformation limit

FRACTURE CORRELATION. The plate fracture test data is plotted in Figure 5. In this figure plate strain energy absorbed to the point of fracture per unit plate area defined by

$$S = \frac{4h}{\pi^2} \left( 1 + \frac{a}{b} \right) F_y e_F \quad (20)$$

is plotted versus mine blast energy flux density,  $E_m$ , where  $E_m$  is

65

## HASKELL

calculated according to Equation 5. Along with the plate test and armored vehicle data points, this figure shows the least squares fit curve of the plate test data,  $2\sigma$  probability limits, and the theoretical fracture line. As in Figure 4 the circles and squares represent 5083 aluminum and class 2 rolled homogeneous armor steel plates respectively. The triangles correspond to actual tank damage from mine blast in South Vietnam. These tank combat data were not used on construction of the test mean. As indicated by the figure the theoretical criterion for fracture is slightly below the test mean line. The average difference between theory and test is -9.4 percent with the average positive and negative differences between theory and test 12.1 percent and 22.2 percent, respectively. The average absolute difference between theory and test is 18.4 percent.

The tank combat damage data points which were not used in arriving at the least squares fit of the data and the  $2\sigma$  limits fall well within the plate test  $2\sigma$  probability limits.

It should be noted that the theory agrees very well with the tank combat damage data points. This agreement, in fact, is within 12 percent.

As in the case of the deformation equation, the fracture relation may be rewritten to allow direct computation of both theoretical and test mean fracture thickness as well as the thickness corresponding to the  $\pm 2\sigma$  probability limits. To this end Eq. 17 is rewritten as follows:

$$h_F = \frac{K E_m}{(1 + \frac{a}{b}) F_y e_F} \quad (21)$$

where

- $K = \pi^2/4$  for the theoretical fracture thickness
- $= 2.868$  for the median test fracture thickness
- $= 1.8056$  for sure fracture, i.e., 95 percent probability of fracture
- $= 3.9306$  for no fracture, i.e., 95 percent probability that fracture will not occur

## V. DISCUSSION

**GENERAL.** Both the deformation relation, Equation 12, and the fracture thickness relation, Equation 17, were derived from first principles without making use of test data to develop the equations. These equations characterize deformation and fracture in terms of plate size, shape and material parameters and mine attack parameters. The deformation equation relates deformation, plate length, width, thickness, and yield strength, mine charge weight and standoff. The fracture equation relates plate width, length, toughness, mine charge weight and standoff with the plate thickness at which fracture occurs. These are all practical factors useful in design and analysis. Furthermore, as formulated, they appear to provide a good characterization of deformation and fracture since predictions of the theoretical deformation and fracture equations correlate within an average error of 18 percent and 10 percent.

HASKELL

respectively with available aluminum and steel plate-mine blast tests and the predictions of the fracture equation correlate within 12 percent with data from armored vehicles damaged by mine blast in combat.

DEFORMATION. Inspection of the deformation equation indicates that, in consonance with experience, deformation decreases as the plate is made more rectangular and as charge weight decreases. It also decreases with increasing plate thickness and yield strength and mine standoff. However, it can be shown that increasing plate thickness above 1 to 2 inches results in only a minor decrease in deformation. It can also be shown that a significant drop in deformation occurs as the yield strength of relatively low strength plate material is increased. On the other hand, the relative decrease in deformation attainable by increasing plate strength above that of class 2 armor steel reaches a point of diminishing returns. For example, to halve the mine blast deformation of present class 2 rolled homogeneous armor steel by increasing yield strength would require a material with a minimum yield strength of approximately 400,000 psi. This is more than twice the nominal value for class 2 armor.

FRACTURE. A relatively simple and straightforward means for determining the thickness of a given plate that will fracture when attacked by a mine blast is provided by nomograms prepared from the fracture equation (Eq. 21) and presented in Reference 6. These nomograms yield mean fracture thickness obtained from test, plate thickness corresponding to 95 percent probability of fracture under mine blast attack, and the plate thickness required for 95 percent probability that the plate will not fracture under mine blast attack. Through five scales these nomograms relate the practical factors: plate width-to-length ratio, toughness, fracture thickness, mine charge weight, and standoff. Fracture thickness can be determined from these nomograms in little more than the time required to draw three straight lines on the nomograms.

Fracture thickness decreases with increasing standoff and toughness and increases with charge weight. For example, doubling standoff from 10 to 20 inches for a 20 lb charge decreases fracture thickness by about 54 percent, or doubling charge weight from 10 to 20 lb almost doubles fracture thickness at a 15 inch standoff. Fracture thickness is heavily dependent on toughness - decreasing hyperbolically with increasing toughness. This behavior is similar to the heavy dependence of deformation on yield strength as described previously. Consequently, the plate fracture thickness-toughness relationship has two practical bounds. One of these is the practical lower toughness bound. Toughness decreases below this bound cause an inordinate rise in plate thickness required to preclude fracture. The other bound is a practical minimum plate thickness bound. To decrease fracture thickness below this practical bound requires a practically unattainable increase in material toughness. For example, if a 5083-H321 aluminum alloy plate with toughness = 3480 in-lb/in.<sup>3/2</sup> is changed to a MIL-T-9046 Type III titanium alloy plate with a 3.7 times the 5083-H321 toughness, the fracture thickness also drops by a factor

## HASKELL

of four. However, for increased toughness beyond that of titanium and class 2 rolled homogeneous armor steel, fracture thickness decreases at a much reduced rate. That is, increasing toughness 64 percent, for example, beyond that of class 2 RHA steel results in only a 35 percent decrease in fracture thickness. This is significant because toughness increases of this magnitude do not appear feasible with present technology.

APPLICATIONS. Figures 6 and 7 illustrate some applications of the deformation and fracture analyses developed by this investigation. These figures are based on Equations 19 and 21 and present the characteristics of a 71 in. by 125 in. plate typical of the size of the bottom hull plate of a current armored vehicle.

Figure 6 shows the effects of plate thickness and mine charge weight on the maximum deformation of both aluminum and steel plates at a typical 17 in. standoff. In consonance with experience, this figure indicates that the steel plates deform much less than the aluminum. For example, the deformation of a 2 in. thick rolled homogeneous armor steel plate attacked by a 10 lb mine is a little less than half the 17 inch deformation of an equal thickness aluminum plate. It may also be noted that the charge weight required to obtain a given level of deformation increases essentially linearly with plate thickness.

Figure 7 illustrates the effect of charge weight, standoff, and plate material on mean fracture thickness, areal weight, and total weight of the typical 71 in. by 125 in. armored vehicle bottom plate. As indicated, mean fracture thickness increases practically linearly with charge weight over the range shown and decreases with increasing standoff. It may also be shown that the charge weight required to fracture a plate of given thickness increases exponentially with standoff. As is well known, the figure illustrates the fact that a considerably thinner steel armor plate is required to defeat a given mine attack than is required by an aluminum plate. For example, the fracture thickness of a class 2 RHA steel armor plate attacked by a 10 lb charge at 17 inches standoff is approximately 1/2 inch compared to approximately 2-1/2 inches for a 5083 aluminum plate. Or, demonstrated in another way, only a 4 lb charge will fracture a 1 inch 5083 aluminum plate at 17 inches standoff whereas approximately 22 lbs is required for a class 2 rolled homogeneous steel armor plate. This is roughly a 5.5 to 1 required charge weight advantage for class 2 steel armor over aluminum plate. However, as shown in the figure, the areal weight of the 1 inch aluminum plate is only 14 lbs/ft<sup>2</sup> whereas the 1 inch steel armor plate weighs about 40 lbs/ft<sup>2</sup>, or three times as much. On an equal weight basis steel armor still has an advantage over aluminum. To demonstrate this consider that \$50 lbs can be allotted to armor the 71 in. by 125 in. bottom of a certain armored vehicle to mine blast attack at 17 inches standoff. This corresponds to approximately a 1 inch thick 5083 aluminum plate. This 1 inch 5083 plate provides protection against fracture from mines containing up to 4 lbs of explosive charge as shown in Figure 7. For this same \$50 lbs a 1/4 inch class 2 RHA steel plate can be employed which will provide protection against mines weighing up to 6 lbs. However, these considerations

HASKELL

have not included a significant conventional vehicle engineering design factor - the static elastic structural stiffness. Even though the 1 inch thick aluminum bottom plate affords only 70 percent as much mine protection as the equal weight 1/4 inch steel plate, it is approximately 21 times stiffer in the elastic service design regime. This discussion serves to illustrate the complexity of armored vehicle bottom plate design but also points up the importance of the deformation and fracture analysis methods developed by this investigation. These methods are particularly suitable for rapid and easy design tradeoffs.

V. SUMMARY AND CONCLUSIONS

Two equations have been developed, one for deformation and one for fracture of flat rectangular simply supported plates subjected to blast attack from shallow-buried mines.

These equations are found to be reasonably accurate for both aluminum and steel plates. Furthermore, the fracture equation yields predictions in good agreement with aluminum and steel armored vehicles damaged by mines in combat. The average error between theoretical deformation predictions and plate test results is +18 percent with the average absolute error 21 percent. The average error for the fracture equation is -9 percent with the average absolute error 18 percent. In addition, predictions of the fracture equation agree within 12 percent with the data from armored vehicles damaged by mine blast in combat.

Present class 2 rolled homogeneous steel armor represents nearly the practical optimum blast attack resistant armor with regard to strength and toughness. Armor materials with greater strength and toughness than class 2 armor do not promise large increases in mine protection commensurate with the probable effort required to achieve the necessary higher strength and toughness.

Plate deformation decreases with decrease in plate aspect ratio, i.e., the ratio of width to length, and it decreases hyperbolically with increasing thickness and yield strength while fracture thickness decreases hyperbolically with plate toughness. Increasing mine charge weight increases deformation exponentially while both deformation and fracture thickness decrease exponentially with increasing mine standoff. Mine charge weight to produce a given amount of deformation increases essentially linearly with plate thickness; and charge weight required to fracture a plate of given thickness increases exponentially with standoff.

The equations developed are directly applicable to the design of munitions and armor and the vulnerability analysis of armor plate subjected to mine blast attack.

69

HASKELL

VI. REFERENCES

1. Rudnick, J., "Static Test of Gunfire Test Boxes Damaged by Internal Blasts," Aero. Strucs. Lab. Nav. Air Exp. Sta., Naval Air Material Center Report No. ASL NAM DE-261, August 1952.
2. Metals Handbook, 8th Ed. Vol. 1, Properties and Selection of Metals, American Society for Metals, T. Lyman, Ed., 1961, pp 108-110.
3. Goodman, H.J., "Compiled Free-Air Blast Data on Bare Spherical Pentolite," Ballistic Research Laboratories, BRL Report No. 1092, February 1960.
4. Adams, C., J. N. Sarmousakis, J. Sperrazza, "Comparisons of the Blast from Explosive Charges of Different Shapes," Ballistic Research Laboratories Report No. 681, Spetember 1948.
5. Makino, R.C. and H.J. Goodman, "Air Blast Data on Bare Explosives of Different Shapes and Compositions," Ballistic Research Laboratories Memorandum Report No. 1015, June 1956.
6. Haskell, D.F., "Deformation and Fracture of Tank Bottom Hull Plates Subjected to Mine Blast," Ballistic Research Laboratories Report to be published.

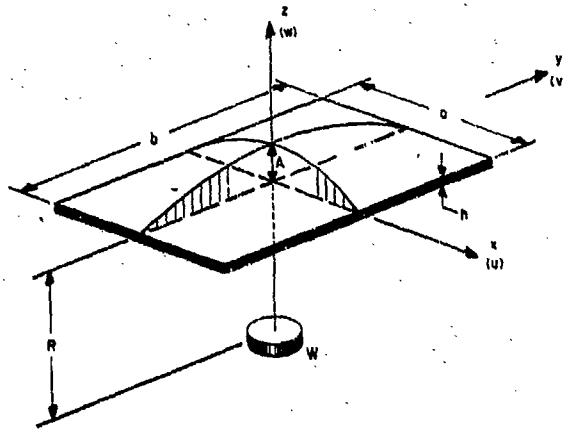


Figure 1 - Mine-Rectangular Plate Configuration

HASKELL

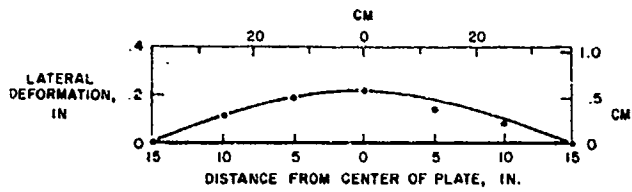


Figure 2. Final Deformation Pattern of a Stiffened Steel Plate Subjected to Confined Air Blast, Data: •

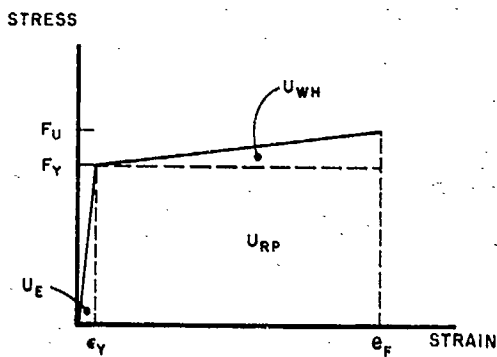


Figure 3. Bilinear Material Stress-Strain Behavior.

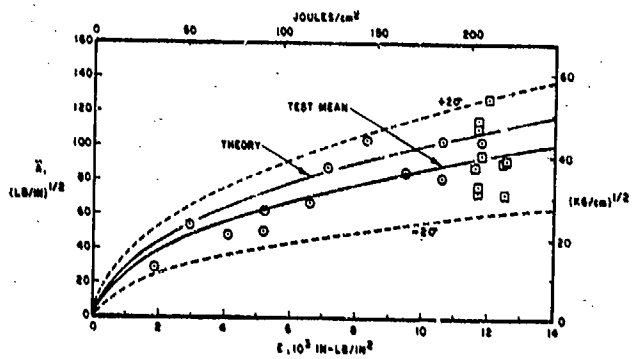


Figure 4. Plate Deformation; O: 5083 Aluminum Test Data, □ Rolled Homogeneous Armor Steel Test Data, —: Least Squares Fit of Data, —: Theory.

HASKELL

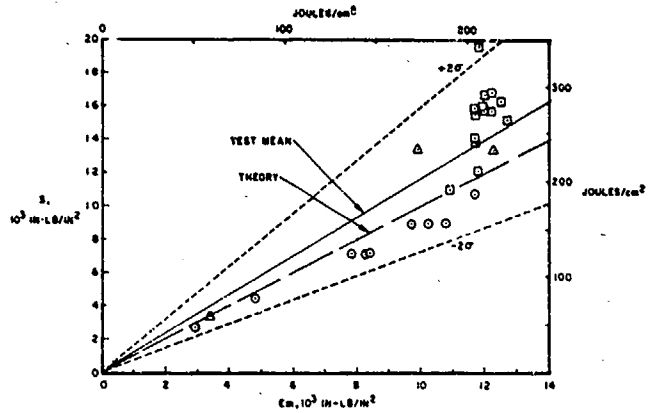


Figure 5 Plate Fracture. 5083 Aluminum Test Data: O, Rolled Homogeneous Armor Steel Test Data: □, Tank Test Data: △, Least Squares Fit of Data: —, Theory: - - -

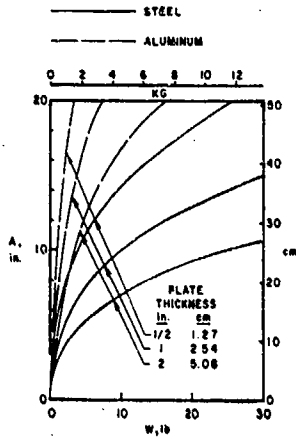


Figure 6 Effect of Thickness and Charge Weight on Deformation of 71in X 125in (1.8m X 3.175m) Class 2 Rolled Homogeneous Armor Steel and 5083 Aluminum Plates at 17in. (43.18cm) Standoff.

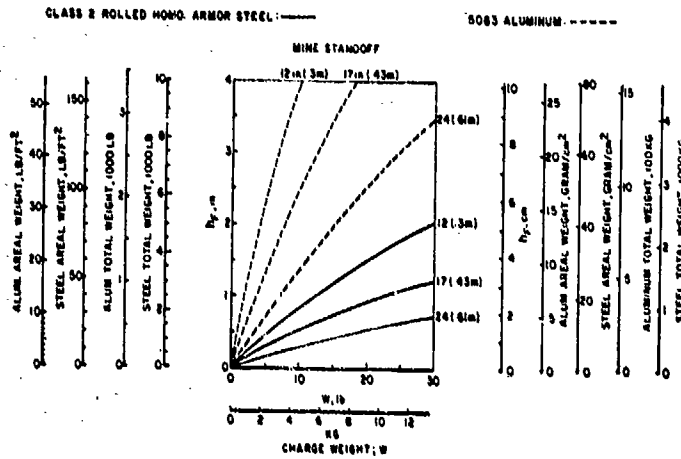


Figure 7 Influence of Charge Weight, Standoff and Material on Mean Fracture Thickness, Areal Weight and Total Weight of 71in X 125in (1.8m X 3.175m) Plate